Global efficiency of power-split hybrid electric powertrain

Antonella Castellano[1] and Marco Cammalleri[1]

[1] Department of Engineering, University of Palermo, Italy
{antonella.castellano,marco.cammalleri}@unipa.it

Abstract. The development of a proper energy management strategy in hybrid electric vehicles is crucial to pursue the best balance between emissions reduction and performance. In this respect, this paper addresses a straightforward method to investigate the behaviour of the hybrid powertrain in steady-state operation in terms of speeds and torques both of the thermal engine and the electric machines. The procedure takes into account the conversion power losses in the internal combustion engine and the electric unit and the mechanical power losses occurring in the power-split transmission. This enables the calculation of a set of maps describing the global efficiency of the hybrid powertrain and the power supplied or gathered by the batteries, which can be exploited in the implementation of a proper control strategy. The proposed approach is based on a unified parametric model that enables a comprehensive analysis of any power-split transmission.

Keywords: SDG13, Hybrid Electric Vehicles, Power-Split CVTs, Powertrain global efficiency.

1 Introduction

The alarming aggravation of global warming has led world leaders to undertake a common commitment by adopting the United Nations Framework Convention on Climate Change (UNFCCC), whose main aim is to decrease the concentration of greenhouse gases in the atmosphere. To accomplish the goals established in the Paris Agreement (2015), relevant environmental policies have been adopted to take urgent action on climate change, by promoting the uptake of zero- and low-emission vehicles, i.e. electric and hybrid electric vehicles.

Among the Hybrid Electric Vehicles (HEVs) architectures, the power-split layout is the most promising one [1-4]. Like any other HEV, the power-split hybrid electric powertrain relies on two different power sources for motion, which are an Internal Combustion Engine (ICE) and an electric unit, which operates as a Continuously Variable Unit (CVU) and consists of two electric machines, power converters and batteries. The deployment of Planetary Gear sets (PGs) and Ordinary Gear sets (OGs), properly arranged in a Power-Split Unit (PSU), enables the decoupling of the thermal engine operation from the wheels speed. Furthermore, not only the ICE power can be used for battery charging as well as for vehicle propulsion, but also the battery pack can supply traction power by cooperating with the ICE or operating in full electric functioning mode.

Typically, low noise, fuel-saving and reduction of CO_2 emissions make the pure electric mode ideal for urban driving, while the involvement of the Internal Combustion Engine (ICE) is more suitable in extra-urban driving. Nonetheless, the system operating point for given vehicle speed and demanded torque should be the one that minimises fuel consumption and optimises global efficiency, according to the current capability of the battery pack of supplying or gathering electric energy. Therefore, proper Energy Management Strategies (EMSs) based on the battery State Of Charge (SOC) have to be implemented to reduce emissions while maintaining driving comfort and high performance [5-7]. For this purpose, the power-split system has to be analysed under various operating conditions.

In this paper, a unified parametric model for Power-Split Continuously Variable Transmissions (PS-CVTs) is applied to perform a comprehensive evaluation of the overall power losses occurring in the powertrain and provide some guidelines to maximise the global efficiency. Any PS-CVT can be preliminarily analysed by the dimensionless method proposed in [8-10], which was expanded and upgraded in [11] and briefly summarised in Section 2. This leads to the calculation of the PSU mechanical power losses and of the subsequent real power flowing into the electric machines. Then, the ICE and electric machines efficiency maps can be introduced to investigate the powertrain behaviour for specific output speed and torque, by assuming proper constraints on the power flowing from or to the battery pack (Section 3). In this way, a global efficiency map can be obtained for every vehicle speed in steady-state operation. Therefore, it is possible to detect the best operating point of the whole system among the feasible ones according to the power that batteries can supply or receive. As a case study, the output-split transmission designed in [12] is analysed in Section 4.

2 Unified parametric model for PS-CVTs

According to the parametric model addressed in [8-11], any PSU can be modelled as a black box with two Degrees Of Freedom (DOFs) and four external ports linked to the ICE (shaft *in*), the wheels (*out*), and the two electric machines (*i* and *o*), as it is shown in Fig. 1a. The PSU can consist of any number of PGs and OGs, arranged in one or more basic structure called Three-Port Mechanisms (TPMs). As Fig. 1b shows, each TPM consists of a PG and up to three OGs, which connect the PG branches (*R*, *S*, *C*, indicated by *X*, *Y*, *Z* in a general way) and the PSU main shafts (*in*, *out*, *i*, *o*, …, indicated by *x*, *y*, *z*). This schematisation enables the utilization of some general equations (not reported here for brevity) based on basic functional parameters, which can be derived from the transmission constructive layout in an analysis phase [11] or properly selected during the design [8,12].

The dimensionless approach outlined in this section is focused on analysis purpose and is suitable even for addressing multi-PG and multi-mode PS-CVTs. All the relationships describing the two-DOF system are normalised to ICE speed, torque and power, so as to reduce the mathematical treatment to a one-DOF problem. For brevity,

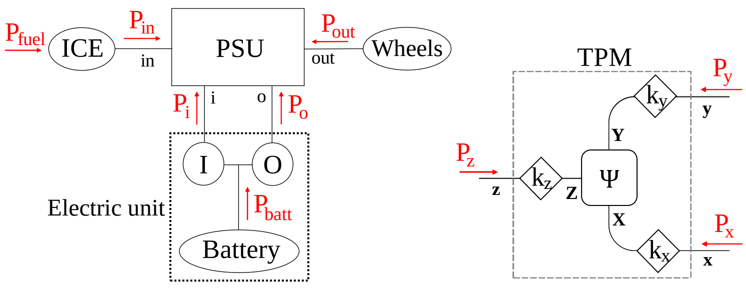

(a) (b)

Fig. 1. Scheme of the power-split powertrain **(a)** and a generic TPM **(b)** with positive power flows direction.

only the main, necessary equations are reported in the following. Further explanations can be found in the previous papers [8-11]. It is worth noting that the model can be swiftly rearranged to study also the full electric operation, as it is addressed in [11].

The whole model relies on some functional parameters that rule PSU speeds, torques and power flows, as well as mechanical power losses. These functional parameters are the nodal ratios and the corresponding speed ratios. The former, indicated as $\tau_{\#k}$, are the overall transmission ratio $\tau = \omega_{out}/\omega_{in}$ achieved when a generic kth shaft is motionless. The latter, indicated as $\tau_{j\#k}$, are the jth speed ratio $\tau_j = \omega_j/\omega_{in}$ calculated for the kth nodal ratio. The procedure for identifying these functional parameters starting from the PSU constructive arrangement is described in [11] and relies on some simple matrix operations performed on a constraints matrix whose rows encloses all the kinematic constraints due to PGs and OGs.

One of the strengths of this model is the simplicity in the calculation of the mechanical power losses occurring in the PSU, applicable to any PS-CVT, constructive layout notwithstanding [10,11]. Once known the constructive ratio and the efficiency of PGs and OGs and calculated the functional parameters, the mechanical power losses occurring in the PSU can be computed as a function of the overall transmission ratio τ and the opposite of the power ratio $\eta = -P_{out}/P_{in}$ (note that η is not the global efficiency, but it considers the possibility for batteries to be charged or discharged). Fig. 2 shows the map of the total mechanical power losses $\bar{p}_L$ normalised to the ICE power calculated by applying the procedure described in [10,11] to the transmission analysed in Section 4.

Once computed the map of the PSU power losses, the real mechanical power flowing through the shaft o can be calculated by the following equation:

$$\bar{p}_o = p_o - \frac{\tau_o}{\tau_{o_{\#i}}}\left[\bar{p}_L + \left(\frac{\partial \bar{p}_L}{\partial \tau} + \frac{\partial \bar{p}_L}{\partial \eta}\frac{\eta}{\tau}\right)(\tau_{\#i} - \tau)\right] \quad (1)$$

where:

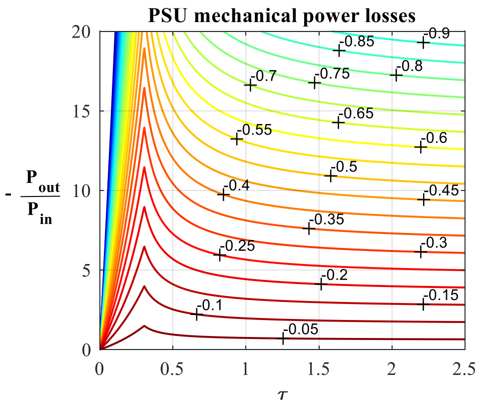

Fig. 2. Example of PSU mechanical power losses $\bar{p}_L$ as a fraction of the ICE power.

$$\tau_o = \frac{\omega_o}{\omega_{in}} = \tau_{o\#i} \frac{\tau - \tau_{\#o}}{\tau_{\#i} - \tau_{\#o}} \tag{2}$$

$$p_o = \frac{P_o}{P_{in}} = \frac{(\tau - \tau_{\#o})(\tau - \eta\, \tau_{\#i})}{\tau(\tau_{\#o} - \tau_{\#i})} \tag{3}$$

From Eq. (1) the real torque on the shaft *o* normalised to T_{in} can be obtained by dividing it by Eq. (2). Analogous relationships are obtained for the shaft *i* by switching the subscripts *i* and *o* in Eqs. (1), (2) and (3).

3 Global efficiency evaluation

The dimensionless approach summarised in Section 2 enables the comprehensive analysis of the PSU response once freely assumed a speed ratio and a power or torque ratio between any two external PSU shafts. Nonetheless, the overall speed ratio τ and the overall power ratio η were chosen as independent variables for convenience. Indeed, the output speed ω_{out} is directly related to the vehicle speed and the output torque supplied to the wheels results in acceleration, deceleration or steady-state operation. In the latter case, P_{out} is dependent on the vehicle speed V_{veh} as follows:

$$P_{out} = -(mg \sin\alpha + f_r mg \cos\alpha + 0.5 \cdot C_d A_f \rho_a V_{veh}^2) V_{veh} \tag{4}$$

P_{out} is negative because it is delivered by the PSU. In Eq. (4), m is the vehicle mass, g is the gravitational acceleration, α is the road slope expressed in radians, f_r is the rolling resistance coefficient, c_x is the drag coefficient, A_f is the vehicle frontal area and ρ_a is the air density.

For each vehicle speed, the PSU can be analysed by imposing proper values for τ and η. In other words, the rotational speed and the real mechanical power of the electric machines can be calculated once fixed the ICE functioning point in terms of ω_{in} and T_{in}. Since the aim of the study is to find the system operating point that maximises the global efficiency, for fixed V_{veh} it is necessary to explore all the feasible ICE functioning points, which are represented in the ICE efficiency map (Fig. 3a). Thus, for each couple of ω_{in} and T_{in}, the calculation of P_{in} is straightforward, along with the identification of the ICE efficiency η_{ICE}. Therefore, the power that has to be provided by fuel combustion is:

$$P_{fuel}(\omega_{in}, T_{in}) = P_{in}/\eta_{ICE} \tag{5}$$

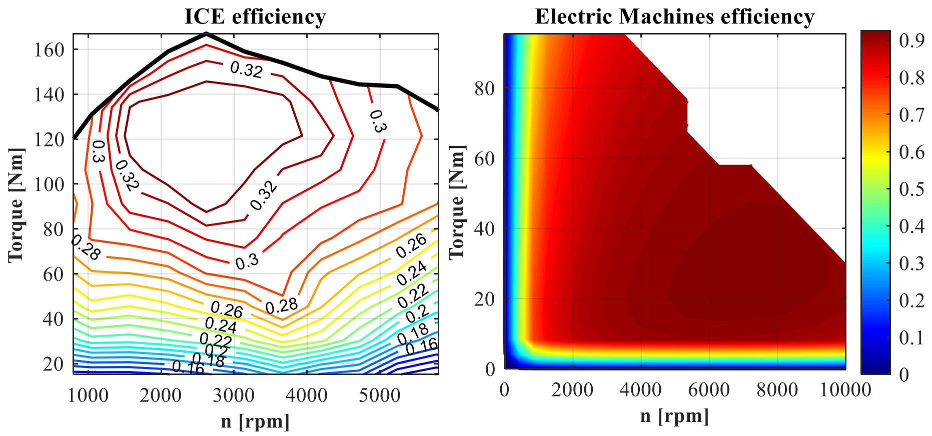

(a) (b)

Fig. 3. Typical ICE efficiency map **(a)** and Electric Machines efficiency map **(b)**.

The rotational speed of the shafts i and o can be computed from Eq. (2) by imposing $\tau = V_{veh}/(R_{wheel} \cdot \omega_{in})$, where R_{wheel} is the wheel radius. Similarly, the powers $\overline{P}_o$ and $\overline{P}_i$ flowing through the shafts i and o can be derived from Eq. (1) and the real torques $\overline{T}_o$ and $\overline{T}_i$ can be obtained by dividing them by ω_o and ω_i. Thus, the respective electric powers $\overline{P}_{o,el}$ and $\overline{P}_{i,el}$ can be computed from the electric machines efficiency map, which indicates the efficiency of the electric machines as a function of torque and rotational speed (Fig. 3b). The net power flow that involves the battery pack is the sum of $\overline{P}_{o,el}$ and $\overline{P}_{i,el}$.

$$P_{batt}(V_{veh}, \omega_{in}, T_{in}) = \overline{p}_o P_{in} \eta_O^{-sign(\overline{p}_o)} + \overline{p}_i P_{in} \eta_I^{-sign(\overline{p}_i)} \tag{6}$$

P_{batt} is positive if batteries provide electric power for vehicle propulsion, while it is negative during battery charging. Therefore, in the former case P_{batt} is an input power provided to the powertrain, along with P_{fuel}. Instead, in the latter case P_{batt} is an output power, similarly to P_{out}. Hence, by defining the powertrain global efficiency η_{gl} as the negative ratio between the total output power and the total input power, two definitions are possible according to the direction of the battery power flow:

$$\eta_{gl}(V_{veh}, \omega_{in}, T_{in}) = -\frac{P_{out}}{P_{fuel} + P_{batt}} \qquad for\ P_{batt} > 0 \tag{7}$$

$$\eta_{gl}(V_{veh}, \omega_{in}, T_{in}) = -\frac{P_{out} + P_{batt}}{P_{fuel}} \qquad for\ P_{batt} < 0 \tag{8}$$

The relationships presented in this section lead to a global efficiency map as a function of ω_{in} and T_{in} for a given vehicle speed. Thus, it is possible to identify the system operating point that achieves the highest efficiency. Nonetheless, the best solution should be selected only among the feasible ones, since the speed and the torque of ICE and electric machines must be comprised between the respective minimum and maximum values.

3.1 Battery State Of Charge

Even the battery power flow cannot exceed a maximum limit both in the charging and discharging phase, according to the current SOC. However, the exact instantaneous SOC is not evaluated in this paper, but four general working conditions are outlined.

If it is supposed that the current SOC is the one that always allows the achievement of the best operating condition, the battery can instantaneously receive or provide any amount of power, so long as it is comprised between the viable constructive limits. In Section 4 we refer to this condition as $SOC = FREE$ and it must be:

$$P_{max\_charge} \leq P_{batt} \leq P_{max\_discharge} \tag{9}$$

The condition whereby the battery is completely charged and thus prevented from receiving further power is indicated as $\mathrm{SOC} = 1$ and implies $P_{max\_charge} = 0$. On the contrary, if the battery is fully discharged ($\mathrm{SOC} = 0$), it cannot supply power and hence $P_{max\_discharge} = 0$. Lastly, the SOC can be maintained constant if $P_{batt} = 0$.

4 Application

The procedure described in the previous sections can be applied to any PS-CVT. In this section, the output-split transmission designed in [12] by the same parametric model is analysed. Its design was aimed at minimising the size of the electric machines, by assuming the vehicle parameters of Table 1, but any power losses were neglected. The ICE can operate between 800 and 5800 rpm, as its efficiency map shows (Fig. 3a), and has 80 kW maximum power. The electric machines have the same size and can deliver up to 35 kW each. The maximum power flow that the battery pack can deliver or receive is 70 kW. The efficiency map of Fig. 3b is used for both electric machines and both for generating and motoring operation.

Table 1. Vehicle parameters.

m [kg]	α [rad]	f_r [-]	c_x [-]	A_f [m^2]	ρ_a [kg/m^3]
2200	0	0.0122	0.4	2.5	1.225

Firstly, the transmission is analysed by the dimensionless method of Section 2. The constructive layout of the transmission, shown in Fig. 4, is derived from [12], as also its basic functional parameters, which are $\tau_{\#o} = 0.218$, $\tau_{\#\mathrm{i}} = \tau_{\mathrm{o}\#i} = -\infty$, $\tau_{\mathrm{i}\#o} = 1.22$.

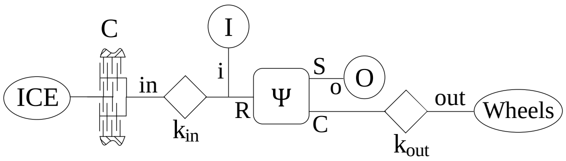

Fig. 4. Transmission functional layout. The clutch C provides full electric operation if engaged.

The PG Willis’ ratio is $\Psi = -0.4$, while the OGs fixed ratios are $k_{in} = \omega_{in}/\omega_R = 0.82$ and $k_{out} = \omega_{out}/\omega_C = 0.25$. The dimensionless mechanical power losses occurring in the PSU are those shown in Fig. 2 evaluated by considering the OGs efficiency equal to 0.98 and the PG fixed-carrier efficiency equal to 0.96. We refer the reader to [10] and [11] for more details. Once computed $\bar{p}_L$, $\bar{p}_o$ and $\bar{p}_i$ are calculated by Eq. (1).

The procedure described in Section 3 is performed for a vehicle speed ranging from 0 to 200 km/h, thus for each V_{veh} a powertrain global efficiency map is obtained. Correspondingly, each system operating point involves a univocal P_{batt}. Therefore, the selection of the best operating point can be performed among the viable functioning points according to the SOC constraints addressed in Section 3.1. It is worth noting that the efficiency of power converters and batteries is not considered here. However, it would have affected the calculation of the only P_{batt}.

4.1 Results and discussion

Fig. 5 shows the results of the simulation, in terms of the best global efficiency achievable for given SOC constraint (Fig. 5a) and the P_{batt} (Fig. 5b), ICE operating point (Fig. 5c) and ICE power (Fig. 5d).

The results show that the absence of instantaneous constraints on the SOC would realise the most efficient power operations while the ICE is on. This is due to the fact that electric machines can simultaneously operate both as motors or as generators, by avoiding power recirculation in the electric unit (the trend of electric machines power is not reported for brevity). Nonetheless, the global efficiency is lower than 0.3 up to 44 km/h, therefore it would be more convenient to turn off the engine and enable the full electric driving if batteries are charged (SOC = 1). Otherwise, if the engine is on also for the lowest speed, it should operate in its maximum efficiency region (Fig. 5c), provided that it is possible to recharge the batteries. However, Fig. 5a suggests that the

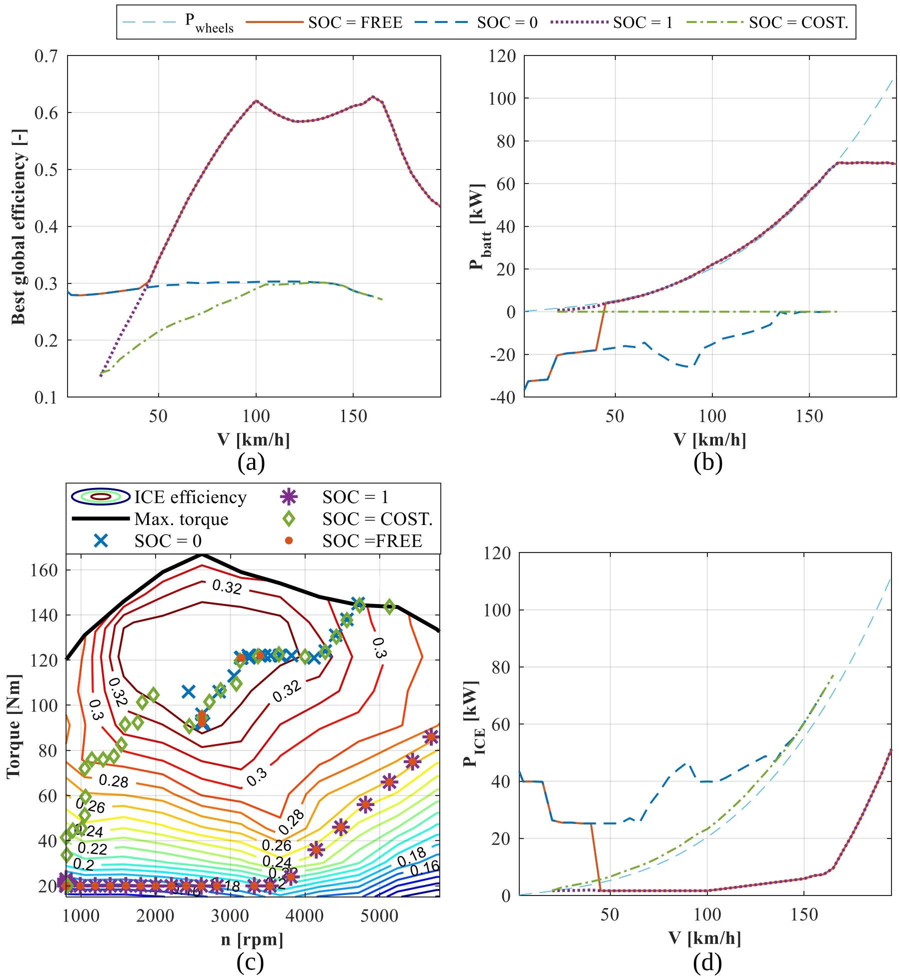

Fig. 5. Simulation results.

battery recharging is more convenient between 65 and 130 km/h because the global efficiency would be slightly higher than the one achievable for lower speeds.

For a medium-high vehicle speed (from 45 km/h), Fig. 5b and Fig. 5d show that the most efficient functioning condition is keeping the ICE at its minimum power and exploit battery power for traction. However, in a real-time optimisation strategy, the battery power flow should be adjusted according to the actual SOC and predicted path, in order to have sufficient range. Therefore, up to 105 km/h, it would be advisable to discharge batteries or recharging them only if $SOC = 0$, but imposing $SOC = COST$ should always be avoided since power recirculation in the electric unit cannot be prevented. Instead, pursuing the most efficient powertrain operations for speeds higher than 105 km/h could result in a very limited range during cruising. Thus, it could be even more advisable to maintain constant SOC from 105 to 135 km/h or increase the ICE power and recharge the battery, while battery charging over 135 km/h should be avoided.

Starting from 165 km/h, the optimal demanded power is higher than $P_{max\_discharge}$, therefore the ICE has to increase its power and thus its losses, which lower the maximum global efficiency. Moreover, since the ICE maximum power is 80 kW the vehicle speed cannot exceed 165 km/h if the batteries are fully discharged ($SOC = 0$) or if a constant SOC is desired.

5 Conclusions

This paper presented a non-iterative approach to provide valuable data that can be exploited for the implementation of a proper EMS, by evaluating the response of a power-split hybrid powertrain in steady-state driving.

The addressed procedure is based on a parametric model that is extremely general and thus suitable for analysing any PS-CVT. It enabled the calculation of a set of maps for every vehicle speed, which includes the feasible operating points of each power source and the trend of the overall powertrain efficiency, as well as the battery power flow. Hence, a real-time control strategy could rely on these results that can be preliminarily computed for reducing the computational burden.

Even though the main goal of this paper was not providing an EMS, the results of the proposed case study suggested that the battery SOC should be maintained always between its minimum and maximum values. In this way, power recirculation in the CVU could be prevented and the overall global efficiency could be maximised. Moreover, in contrast to many rule-based strategies [6,13], it is not always advisable to let the ICE work within its maximum efficiency region if the final aim is minimising the power losses of the whole powertrain, similarly to [14].

It should be noted that the procedure here implemented for a vehicle in specified steady-state operation (i.e., for fixed on-board load and road slope) could be swiftly replicate for any other vehicle under different conditions, by simply considering different vehicle parameters and transmission, as well as propulsors efficiency maps.

Future works might extend this research in order to investigate the powertrain behaviour in dynamic operation, by taking into consideration the inertia of vehicle and propulsors to evaluate the maximum acceleration available or embed a real-time control strategy by taking into account the instantaneous battery SOC.

References

1. Mi, C., Masrur, M. A.: Hybrid Electric Vehicles, Principles and Applications with Practical Perspectives. 2nd ed. WILEY (2017).
2. Zhuang, W., Li, S., Zhang, X., Kum, D., Song, Z., Yin, G., Ju, F.: A survey of powertrain configuration studies on hybrid electric vehicles. Appl. Energy 262, 114553 (2020).
3. Singh, K. V., Bansal, H. O., Singh, D.: A comprehensive review on hybrid electric vehicles: architectures and components. J. Mod. Transp. 27(2), 77–107 (2019).

4. Cammalleri, M, Sorge, F.: Approximate Closed-Form Solutions for the Shift Mechanics of Rubber Belt Variators." Proceedings of the ASME International Design Engineering Technical Conferences and Computers and Information in Engineering Conference 2009, DETC2009 6, pp. 187-196. https://doi.org/10.1115/DETC2009-86638.
5. Zhang, F., Wang, L., Coskun, S., Pang, H., Cui, Y., Xi, J.: Energy Management Strategies for Hybrid Electric Vehicles: Review, Classification, Comparison, and Outlook. Energies 13 (13), 1–35, 2020.
6. Zhang, P., Yan, F., Du, C.: A comprehensive analysis of energy management strategies for hybrid electric vehicles based on bibliometrics. Renew. Sustain. Energy Rev. 48(205), 88–104 (2015).
7. Panday, A., Bansal, H. O.: A Review of Optimal Energy Management Strategies for Hybrid Electric Vehicle. Int. J. Veh. Technol. 2014, 160510 (2014).
8. Cammalleri, M., Rotella, D.: Functional design of power-split CVTs: An uncoupled hierarchical optimized model. Mech. Mach. Theory 116, 294–309 (2017).
9. Rotella, D., Cammalleri, M.: Direct analysis of power-split CVTs: A unified method. Mech. Mach. Theory 121, 116–127 (2018).
10. Rotella D., Cammalleri, M.: Power losses in power-split CVTs: A fast black-box approximate method. Mech. Mach. Theory 128, 528–543 (2018).
11. Cammalleri, M., Castellano, A.: Analysis of hybrid vehicle transmissions with any number of modes and planetary gearing: kinematics, power flows, mechanical power losses. Mech. Mach. Theory 162, 104350 (2021).
12. Rotella, D., Cammalleri, M., Qin, D., Zhou, X.: A Simple Method for the Design of Hybrid Electric Power-Split CVTs: A Case Study. In: Carbone G., Gasparetto A. (eds) Advances in Italian Mechanism Science. IFToMM ITALY 2018. Mechanisms and Machine Science 68. Springer, Cham (2019).
13. Banvait, H., Anwar, S., Chen, Y.: A Rule-Based Energy Management Strategy for Plug-in Hybrid Electric Vehicle (PHEV). 2009 American Control Conference, 3938–3943 (2009).
14. Ahn, K., Cho, S., Cha, S. W., Lee, J. M.: Engine operation for the planetary gear hybrid powertrain. Proc. Inst. Mech. Eng. Part D J. Automob. Eng. 220(12), 1727–1735 (2006).